

Study of tetracene thin film transistors using La_2O_3 as gate insulator

R Sarma* & D Saikia

Thin Film Lab, Department of Physics, J B College, Jorhat, Assam

*E-mail: sarmamax2000@yahoo.com

Received 8 June 2009; revised 28 August 2009; accepted 30 September 2009

Tetracene organic field-effect transistors (OFET) have been fabricated and investigated with La_2O_3 as gate insulator. The fabricated organic thin film transistors exhibit *p*-type conductivity with field effect mobility $1.04 \times 10^{-4} \text{ cm}^2/\text{V.s}$, ON-OFF ratio 3.465, sub-threshold swing 17.8 mV/decade and hole concentration $1.25 \times 10^{19} \text{ cm}^{-3}$. The SEM and XRD analysis on the semiconductor film were also reported.

Keywords: Organic thin film transistors, Tetracene, Gate insulator, Hole concentration, Interface traps

1 Introduction

Organic thin film transistors (OTFT) have gained much interest in recent years due to their flexibility, low cost and easy processing. OTFTs have many electronic applications, such as information display¹, chemical sensors^{2,3}, electronic paper⁴ and microelectronics^{5,6}. The OTFTs can be fabricated by using the simple techniques of vacuum evaporation⁷ and spin coating. The development of OTFTs is hindered by the poor performance of the device over conventional Ge and Si-TFTs⁸. In this paper tetracene is used as organic semiconductor and La_2O_3 as gate insulator. Anderson⁹ pointed out that the useful guide to a good insulator is to choose one with low optical absorption i.e. one which is colourless and transparent in the film form. La_2O_3 film is transparent and it has high thermal and chemical stability, high resistivity and low dielectric loss.

2 Experimental Details

The OTFTs were fabricated in staggered electrode structure (Fig. 1). In this structure the metal (Al) source and drain electrodes, with a channel of length 50 μm between them defined by a wire grill, were first deposited on to chemically and ultrasonically cleaned glass slides.

A semiconductor layer of tetracene followed by an insulator (La_2O_3) was then deposited in steps. Finally a metal (Al) gate electrode was deposited (Fig. 2). The devices were made in a vacuum of better than 8×10^{-6} torr using multiple pump down method. All the materials were properly degassed in vacuum prior to deposition. The various geometrical patterns were defined by metal masks.

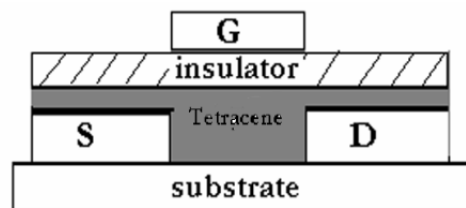


Fig. 1 — A schematic illustration of a tetracene -OTFT configuration

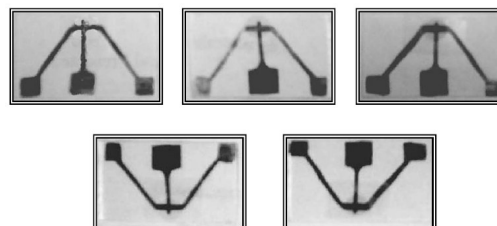


Fig. 2 — Photograph of the fabricated tetracene OTFTs

3 Results and Discussion

Figure 3 shows the plot of drain current I_D vs drain voltage V_D . Here both experimental and theoretical curves are shown. In Fig. 3 the current increases with increasing negative gate voltage. This indicates field-effect-induced hole conduction, which is the expected behaviour for Tetracene. In the linear region of OTFT the drain current is given by¹⁰:

$$I_D = \frac{w}{L} \mu C_i \left(V_G - V_T - \frac{V_D}{2} \right) V_D \quad \dots(1)$$

where w is the channel width, L is channel length, C_i is the capacitance per unit area of the gate insulator, V_T is the threshold voltage and μ is the mobility.

In saturation region $V_D = V_G - V_T$; drain current is given by¹⁰:

$$I_{Dsat} = \frac{w}{2L} \mu C_i (V_G - V_T)^2 \quad \dots(2)$$

Plot of $(I_{Dsat})^{1/2}$ versus V_G is shown in the Fig. 4. The field effect mobility μ is calculated from slope of the linear region of $(I_{Dsat})^{1/2}$ versus V_G graph and the

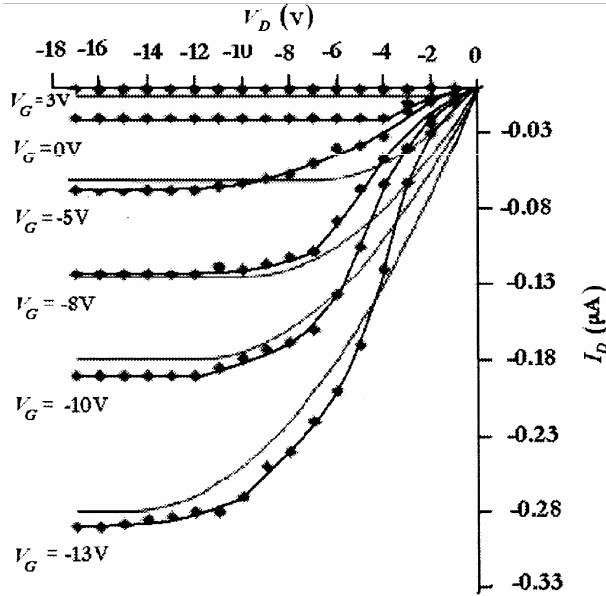


Fig. 3 — Variation I_D versus V_D (the dotted lines indicate the practical variations while the smooth lines indicated the theoretical variations)

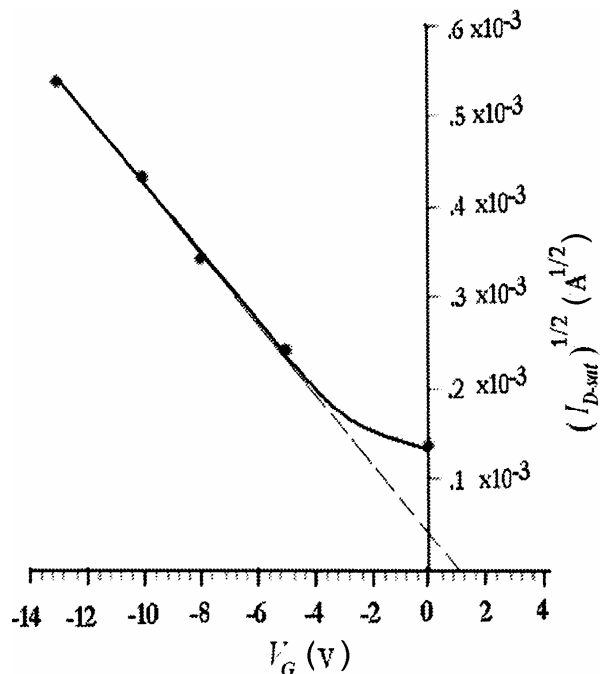


Fig. 4 — Plot of $(I_{Dsat})^{1/2}$ versus V_G

extrapolation of the linear region of the plot to the V_G axis gives the threshold voltage⁹ V_T . As shown in the Table 1 threshold voltage is +1.15V. The positive threshold voltage for p -channel devices may indicate the presence of unwanted n -dopant in the organic layer, thus a positive V_G is needed to switch off the device¹¹. The field effect mobility is $1.04 \times 10^{-4} \text{ cm}^2/\text{V.s}$. The low value of mobility for this small channel OTFT is due to the fact that the molecules of tetracene cannot completely cover the surface of the gate between source and the drain contacts and there exist the voids at the interface between La_2O_3 and tetracene thin film. Thus the portion occupied between voids in the gate area becomes larger for small channel length. Therefore in order to improve the interface property one should use the derivatives of tetracene exhibiting an enhanced adhesion to La_2O_3 . Those treatments are under study.

Plot of $\log(I_D)$ versus V_G at a constant drain voltage (15 V) is shown in the Fig. 5. The sub-threshold swing is calculated from the slope of this graph using the relation¹²:

Table — Various parameters used and evaluated

Channel width (w)	0.16 cm
Channel length (L)	0.005 cm
Capacitance per unit area (c_i)	0.009 F/m ²
Channel thickness (d)	1300 Å
Threshold voltage (V_T)	1.15 V
Channel Mobility (μ)	$1.04 \times 10^{-4} \text{ cm}^2/\text{V.s}$
Channel Conductivity (σ)	$2.04 \times 10^{-4} \Omega^{-1} \text{ cm}^{-1}$
Sub threshold swing (s)	17.8mV/decade
I_{ON}/I_{OFF}	3.465
Hole concentration (N_p)	$1.25 \times 10^{19} \text{ cm}^{-3}$
Maximum numbers of interface traps present (N_{ss}^{max})	$1.71 \times 10^{12} \text{ eV}^{-1} \text{ cm}^{-2}$

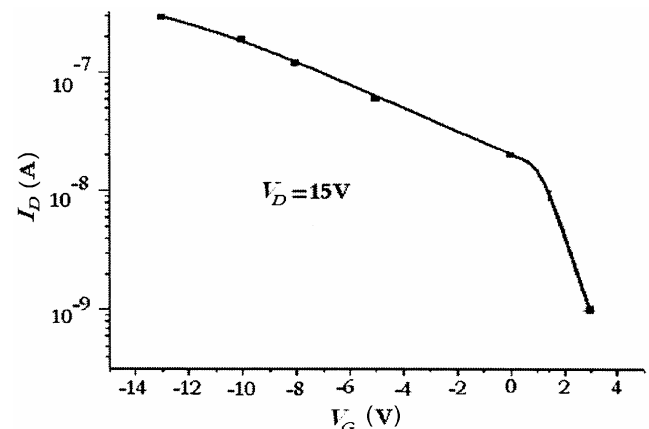


Fig. 5 — $\log_{10}(I_D)$ versus V_G characteristics for the tetracene TFT at $V_D = 15\text{V}$

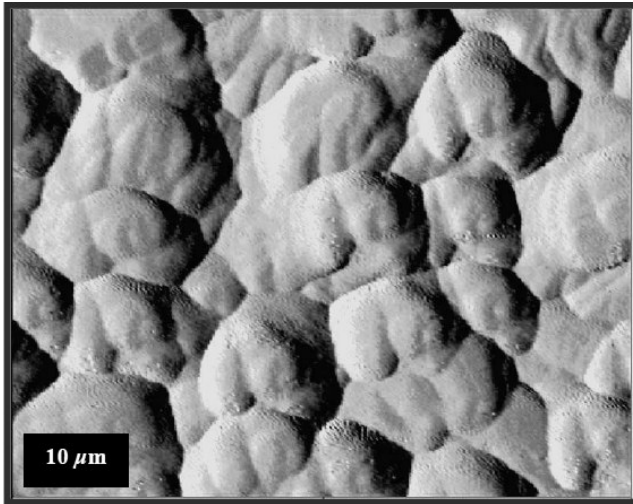


Fig. 6 — SEM image of tetracene thin film on glass substrates

$$s = \left(\frac{d(\log I_D)}{dV_G} \right)^{-1} \quad \dots(3)$$

From the measurement one finds the sub-threshold slope to be 17.8 mV/decade. Normalizing¹³ this value to the capacitance of the dielectric gives 16.02 VnF/decade.cm². These values are comparable to what is found for the best pentacene TFTs^{14,15} [15-80 VnF/decade.cm²]. Further analysis is possible from the sub-threshold slope calculation. The maximum number of interface traps present is estimated using the following relation assuming that the densities of the deep bulk states and interface states are independent of energy^{12,16}:

$$N_{ss}^{\max} = \left\{ \frac{s(\log e)}{KT/q} - 1 \right\} \frac{C_i}{q} \quad \dots(4)$$

The channel conductivity σ is estimated from the plot of I_D versus V_D graph at zero gate voltage.

The ON-OFF ratio is estimated from the following relation¹⁰:

$$\frac{I_{NO}}{I_{OFF}} = \frac{c_i \mu (V_G - V_T)^2}{\sigma d V_D} \quad \dots(5)$$

The surface morphology of the tetracene film is examined with scanning electron microscope (SEM). The tetracene film deposited on the glass substrate is shown in the Fig. 6. This SEM micrograph shows that the tetracene films are polycrystalline in nature and is composed of linear chain of identical crystallites.

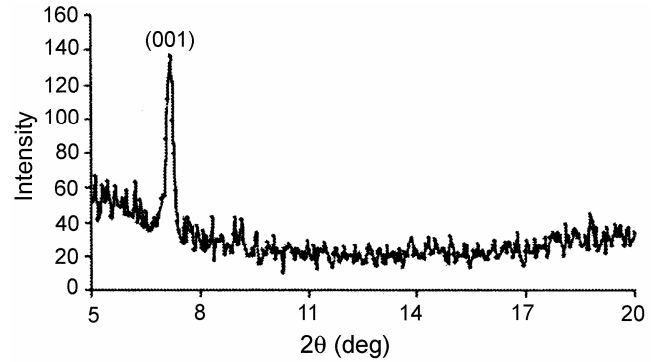


Fig. 7 — XRD pattern of the Tetracene thin film deposited on glass substrate

In Fig. 7, the XRD pattern of tetracene thin film deposited on glass substrate is shown. The observed Bragg's peak (001) shows that thin films of tetracene deposited at room temperature is poly crystalline in nature and consist of only thin film phase¹⁷. It is mainly due to the film deposition at ultrahigh vacuum conditions and at low deposition rate. The peaks indicate that the tetracene molecules are packed parallel to each other in a nearly vertical direction where the c -axis of the tetracene molecule is aligned perpendicular to the substrate¹⁷.

4 Conclusions

Good quality tetracene thin films under optimum vacuum deposition condition are extracted at room temperature with deposition rate 0.3Å /sec. The devices behave as p-channel transistors working in accumulation mode. The fabricated OTFTs have good performance and well defined I - V characteristics. Various parameters evaluated in this work give good understanding study of the OTFT structure.

Acknowledgement

The authors acknowledge University Grant Commission, New Delhi, India for financial support under major research project program.

References

- 1 Mach P, Rodriguez S J, Nortrup R, *et al.*, *Appl Phys Lett*, 78 (2001) 3592.
- 2 Crone B, Dodabalapur A, Gelperin A, *et al.*, *Appl Phys Lett*, 78 (2001) 2229.
- 3 Crone B, Dodabalapur A, Sarpeshkar R, *et al.*, *J Appl Phys*, 91 (2002) 10140.
- 4 Rogers J A, Bao Z, Baldwin K, *et al.*, *Proc Natl Acad Sci USA*, 98 (2001) 4835.
- 5 Crone B K, Dodabalapur A, Sarpeshkar R, *et al.*, *J Appl Phys*, 89 (2001) 5125.
- 6 Klauk H, Gundlach D J & Jackson T. N, *IEEE Electron Device Lett*, 20 (1999) 289.

- 7 Sarma R & Baishya B, *J Instrum Soc India*, 33 (2003) 42.
- 8 Konwar K, Gogoi P & Baishya B, *Indian J Phys*, 80 (2006) 1021.
- 9 Anderson J C, *Thin Solid Films*, 38(1976) 151.
- 10 Shekar B C, Jiyeon Lee & Shi-Woo Rhee, *Korean J Chem Engg*, 21 (2004)267.
- 11 Koch N, *Chem Phys Chem*, 8 (2007) 1438.
- 12 Jung Hoon Seo, Jae-Hong Kwon, *et al.*, *Semicond Sci Technol*, 22 (2007) 1039.
- 13 de Boer R W I, Kalpwijk T M & Morpurgo A F, *Appl Phys Lett*, 83 (2003) 4345.
- 14 Gundlach D J, Nichols J A, *et al.*, *Appl Phys Lett*, 80 (2002) 2925.
- 15 Lin Y Y, Gundlach D J, *et al.*, *IEEE Trans Electron Devices*, 44 (1997) 1325.
- 16 Rollend A, Richard J, *et al.*, *J Electrochem Soc*, 140 (1993) 3679.
- 17 Kang S J, Noh M, Park DS *et al.*, *J Appl Phys*, 95 (2004) 2293.